*Smart Structures and Systems, Vol. 6, No. 2 (2010) 147-165*
DOI: http://dx.doi.org/10.12989/sss.2010.6.2.147


# Experimental studies on impact damage location in composite aerospace structures using genetic algorithms and neural networks

Shahruddin Mahzan, Wieslaw J. Staszewski* and Keith Worden

*Department of Mechanical Engineering, Sheffield University, Mappin Street, Sheffield S1 3JD, United Kingdom*

*(Received April 10, 2008, Accepted October 10, 2009)*

**Abstract.** Impact damage detection in composite structures has gained a considerable interest in many engineering areas. The capability to detect damage at the early stages reduces any risk of catastrophic failure. This paper compares two advanced signal processing methods for impact location in composite aircraft structures. The first method is based on a modified triangulation procedure and Genetic Algorithms whereas the second technique applies Artificial Neural Networks. A series of impacts is performed experimentally on a composite aircraft wing-box structure instrumented with low-profile, bonded piezoceramic sensors. The strain data are used for learning in the Neural Network approach. The triangulation procedure utilises the same data to establish impact velocities for various angles of strain wave propagation. The study demonstrates that both approaches are capable of good impact location estimates in this complex structure.

**Keywords:** composites; aerospace structures; impact damage detection; genetic algorithms; neural networks.

## 1. Introduction

Composite materials have been widely used in many engineering applications due to their high specific strength, light weight and flexibility in design. Good performance displayed by composites has benefited many industries especially in the transportation area. Composite materials, apart from their strength and light weight, also offer resistance to fatigue, corrosion and impact damage. This is particularly important in aerospace engineering.

The susceptibility of composite materials to incur impact damage is well known and creates a major concern related to structural integrity. Low velocity impacts are often caused by bird strikes, tool drops during servicing or runway stones during take off. Such impacts may result in various forms of damage such as indentation, delamination or fibre/matrix cracking, leading to severe reduction in strength and integrity of composite structures. Although structures designed with safe-life principles can withstand in theory catastrophic failures, impact damage detection is an important problem in aircraft maintenance. Visible damage can be clearly detected and remedial action taken to maintain structural integrity. However, a major concern to end-users is the growth of undetected, hidden damage caused by low velocity impacts and fatigue. This undetected, hidden damage is also known in aerospace applications

*Corresponding Author, E-mail: w.j.staszewski@sheffield.ac.uk

as Barely Visible Impact Damage (BVID). Failure to detect BVIDs may result in a catastrophe.

Impact detection is also important in space vehicles which are exposed to many unexpected impact events caused by foreign objects such as falling vehicle's elements, surface debris or micro-meteors. The foam impact that caused the 2003 space shuttle tragedy is a good example. Therefore sensitive and reliable damage detection methods in composite materials are needed to prevent possible damage related problems.

Damage detection in composite materials can be divided into active and passive approaches. The active approach is usually based on various NDT techniques utilising actuators and receivers; examples include various techniques based on ultrasonic, acousto-ultrasonic waves or X-rays. In contrast passive approaches do not involve any actuators; receivers are used to "sense and/or hear" any perturbations caused by possible hidden damage. Various approaches are possible. For example, in impact damage detection sensors are either embedded into or bonded onto structures in order to monitor (i.e. detect and locate) impacts and analyse strain data. The energy of impacts is then estimated using advanced signal processing techniques. It is assumed that certain energy levels can lead to structural damage. This information is possible from material properties and design studies.

Several research investigations related to passive impact damage detection have been performed. Initial studies of acoustic waves produced by low-velocity impacts have been investigated in Gardiner and Pearson (1985). The application of piezoelectric sensors for acoustic wave sensing used in impact detection in impact damage detection has been reported in Weems, *et al*. (1991). Optical fibre sensors have been used for impact damage detection in composite panels in Gunther, *et al*. (1992). Piezopolymer sensors have also been used Hahn, *et al*. (1994) to detect the location and intensity of low-energy impacts in composite panels. This study has involved the application of a binary pattern associator for signal processing. Optical fibre sensors and Artificial Neural Networks (ANNs) have been used in Sirkis, *et al*. (1994) for the position of space debris impacts and to quantify the strain energy absorbed by the space structure as a result of these impacts. The method was validated using isotropic plates. The last two references have initiated a number of studies based on advanced signal processing for impact damage detection. The ANN analysis presented in Sirkis, *et al.* (1994) has been extended to impact detection in composite panels (Schindler, *et al*. 1995). The Levenberg-Marquardt algorithm and the generalisation method were applied within the ANN-based algorithm for impact detection in composite laminates (Sung, *et al*. 2000). Genetic Algorithms (GAs) combined with ANNs have been used for impact detection (Worden and Staszewski 2000). The Multi-Layer Perceptron (MLP) was used to locate impacts positions and quantify their energy in an anisotropic composite panel in this investigation. A similar approach has been applied for optimal sensor location studies in Staszewski, *et al*. (2000). The method presented in Worden and Staszewski (2000), Staszewski, *et al*. (2000) has been automated for impact detection in smart composite panels with embedded piezoceramic sensors (Haywodd, *et al*. 2001, 2005). The MLP-based approached used in (Worden and Staszewski 2000, Staszewski, *et al*. 2000, Haywood, *et al.* 2001, 2005) has been validated in a complex wing-box structure from a commercial aircraft using a regression approach (Le Clerc, *et al*. 2004). An ANN was trained to predict impact coordinates when presented with various signal features. This work has been extended to a classification approach (Le Clerc, *et al.* 2007) in which substructures has been represented by unique class labels. Another impact location approach based on machine learning employs a Case-Based Reasoning (CBR) approach (Mujica, *et al.* 2005, 2006). This methodology creates an initial case-base with principal impact features as a reference. For each impact test, data are diagnosed by analogy with a case base, i.e. reused or revised following the initial knowledge stored in the case-base. Impact location is achieved when similar cases are retrieved.

Feature extraction and dimensionality reduction is important in ANN and CBR based techniques.

Several studies have been performed to investigate this problem. A number of different features obtained from time, spectrum and envelope signals were used as the input for the MLP network in Le Clerc, *et al.* (2004, 2007). Wavelet analysis has also been used for feature extraction, as reported in Sung, *et al.* (2000), Staszewski, *et al*. (1999, 2002), Meo, *et al*. (2005). The studies have allowed for high-frequency features related to damage to be extracted from strain data. The work has involved time-frequency wavelet maps, maximum amplitude from wavelet coefficients and kurtosis. The CBR approach in Mujica, *et al*. (2005, 2006) has been extended in Mujica, *et al*. (2006) to the application of multivariate statistical process control techniques for reducing dimensionality. The study involves linear (principal component analysis) and non-linear (self organising maps and curvilinear distance analysis) techniques.

A modified triangulation procedure was proposed for impact damage detection in composite structures in Coverley and Staszewski (2002, 2003). The method uses experimental velocity characteristics and applies GAs to locate impacts. In contrast to ANN-based approaches the method does not require significant amount of data for training.

A vector-based triangulation procedure for impact location in orthotropic composite materials has been used for impact location in Kessler and Raghavan (2008).

An approach based on system modelling has been proposed in Choi and Chang (1996), Seydel and Chang (1999, 2001), Cardi, *et al.* (2006). The method utilises a structural model which is used to obtained dynamic responses for simulated impact locations. Measured sensor outputs are then compared with the estimated responses from the model. If the two responses are not identical, the algorithm revises the model to characterise the response to a different impact location. This process is iterated until the model response and the actual response of the structure converge. System modelling is not easy for complex structures, and this is the major drawback of the method. Also, the results lead to significant location errors even for simple structures such as beams and plates.

Previous work in this area demonstrates that machine learning techniques are capable of modelling extremely complex relationships between input and output data and produce impressive impact location results even in complex structures (Le Clerc, *et al.* 2004, 2007, Mujica, *et al*. 2005, 2006). However, these methods require a significant amount of impact data for learning and this is not always possible. The optimised triangulation procedure (Coverley and Staszewski 2002, 2003) produces very good results for simple structures and does not require substantial data.

The aim of the current paper is to compare both techniques using a complex composite structure with bonded low-profile piezoceramic sensors. The focus of these investigations is on impact location.

The methods used are briefly described in Sections 2 and 3. The experimental work performed on a composite wing-box structure is presented in Section 4. This involves impact tests and strain wave propagation analysis. Impact location results are presented and compared in Section 5. Finally, the paper is concluded in Section 6.

## 2. Modified multilateration procedure for impact location

The impact location problem can be solved in isotropic materials using classical localisation techniques, such as triangulation, trilateration and multilateration (Mahzan 2007), which require strain data from a set of only three sensors. This approach is clearly not possible for composites which are anisotropic materials. Different frequency components of strain waves propagate in composite materials in different directions with different velocities. However, once velocity characteristics are obtained

experimentally for various angles of wave propagation a simple triangulation procedure with a Genetic Algorithm (GA) optimisation scheme can be used for impact location, as described in Coverley and Staszewski (2002, 2003).

### 2.1. Impact location algorithm

When an impact event occurs, the monitored structure is deflected and strain waves propagate outwards in all possible directions. In other words, the impact is a source of flexural strain waves propagating in the monitored structure and the task is to estimate the position of this source. Three different transducers, namely $S_1$, $S_2$ and $S_3$, can be used to sense the strain, as illustrated in Fig. 1. The waves propagate from the unknown impact position towards these transducers. The procedure selects randomly three different angles, namely $\alpha_1$, $\alpha_2$ and $\alpha_3$, for wave propagation directions. For every transducer $S_i$ and assumed wave propagation angle, the distance $d_i$ between the transducer and unknown impact position can be calculated as

$$d_i = v_i\, t_i \quad \text{(i=1, 2, 3)} \tag{1}$$

where $t_i$ and $v_i$ are arrival times and velocities of the propagating strain waves. The arrival times can be estimated from the experimental strain data for all relevant transducers. The major difficulty is the velocity $v_i$ which depends on the wave propagation direction for anisotropic materials. However, the velocity characteristics $v_i = f(\alpha_i)$ can be estimated a priori for monitored composite structures using experimental analysis for all possible angles of wave propagation.

For the assumed wave propagation directions $\alpha_i$ and estimated distance $d_i$, the analysis of strain data from three different transducers results in three estimated impact positions, i.e. $A_1$, $A_2$ and $A_3$. These positions can be considered as the vertices of a triangle. The GA can be used to minimise the area of this triangle. Finally, the estimate for $x$ and $y$ coordinates of the unknown impact position can be obtained as

$$x = \frac{1}{3}(x_{A_1} + x_{A_2} + x_{A_3}) \quad \text{and} \quad y = \frac{1}{3}(y_{A_1} + y_{A_2} + y_{A_3}) \tag{2}$$

where $x_{A_1}, x_{A_2}, x_{A_3}$ and $y_{A_1}, y_{A_2}, y_{A_3}$ are the $x$ and $y$ coordinates for the $A_i$ ($i$=1, 2, 3) vertices, respectively. The entire procedure, presented graphically in Fig. 2, can be implemented for any configuration of three sensors.

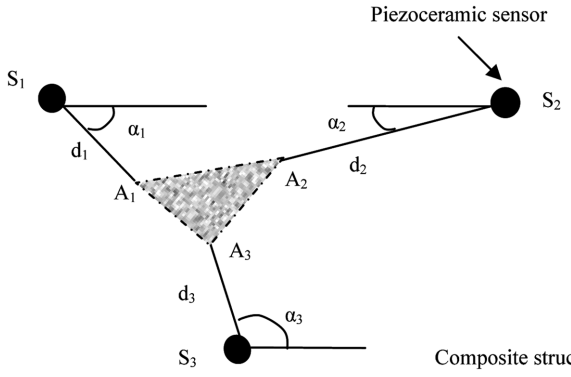


Fig. 1 Illustration of modified triangulation impact location procedure

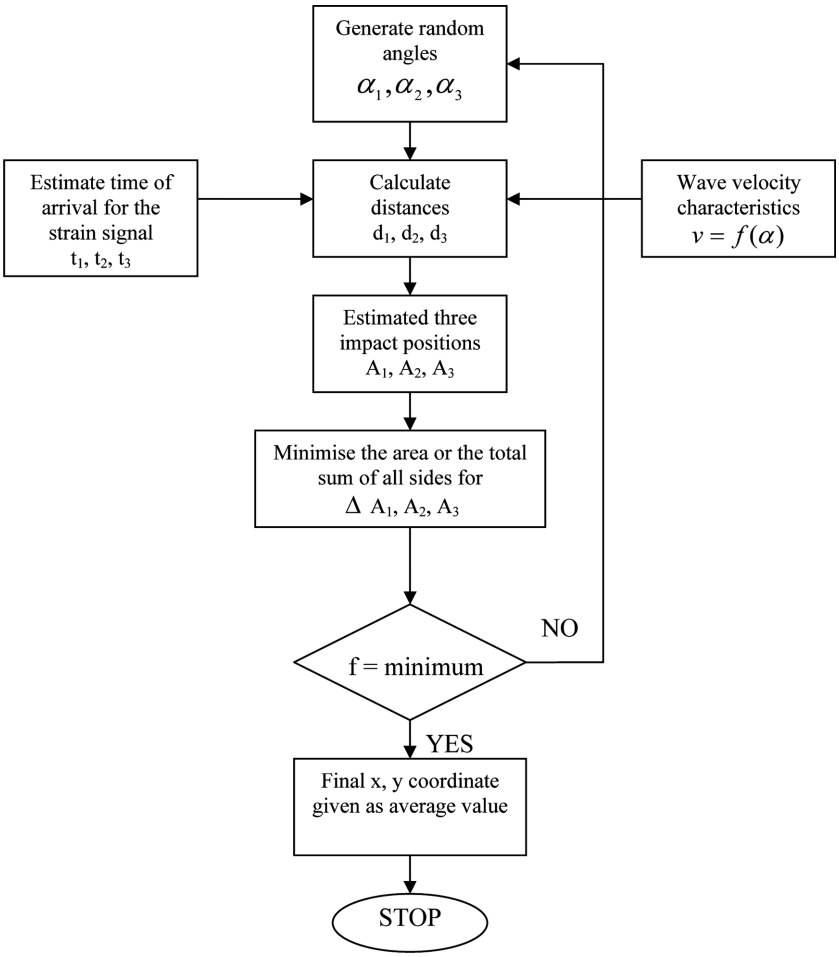


Fig. 2 Modified traingulation/multilateration with a GA optimisation scheme for impact location in composite structure

## *2.2. Genetic algorithms*

This section briefly describes the principles of genetic algorithm. GA is an optimisation algorithm based on the principles of natural selection and natural genetic (Goldberg 1989). This algorithm was developed in the 1970s by Holland (1975). GAs are designed to mimic natural biological evolution, i.e. inheritance, mutation, reproduction and crossover. GAs offer an alternative way to find optimal solutions close in performance to the global optimum (i.e. maximum or minimum) value. The algorithm is simple and robust. GAs can be easily implemented in computer simulations and used for various optimisation problems in order to achieve optimal solutions.

In general, GA operations should follow several steps such as encoding, evaluation, reproduction, crossover and mutation (Goldberg 1989). The GA process starts with random selection over encoded individuals, i.e. finite-length strings using some pre-defined alphabet. This generates an initial population representing a set of possible solutions. There are several types of encoding, i.e. binary, integer, real-values, character-based and list-based rules (Goldberg 1989). However, the binary encoding is the most commonly used due to its simplicity. The next step is the evaluation step, whereby an objective function

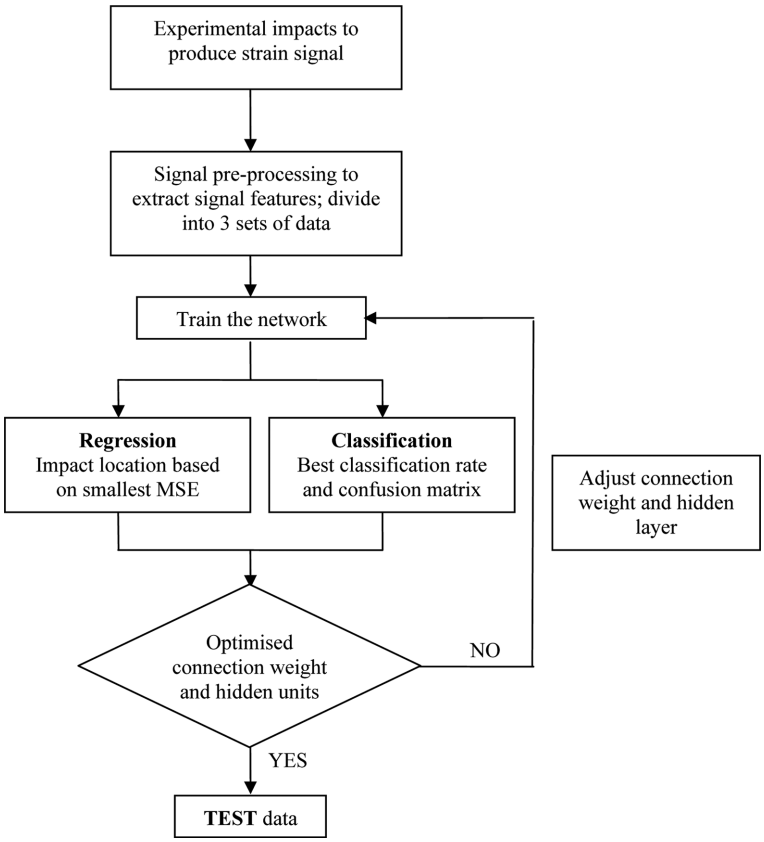


Fig. 3 MLP network procedure for impact location in a composite structure

(often called a fitness function in GAs) is applied to consecutive populations to evaluate its current best solution in order to search for an optimal solution. Reproduction is a copying process to produce a new generation according to the objective function. A modification of the initial population is then made in the next step by introducing operations such as crossover and mutation. Crossover is a process in which old individuals (parents) mate to produce new individuals (children). A mutation process is then performed on child individuals created from the crossover process to prevent premature loss of genes at a particular position. This process is performed by flipping a bit value at a certain position of an individual based on a mutation probability, which decides how often parts of the individual being mutated. The entire process is repeatedly iterated to produce the next population. Finally, after many generations the optimum solution is obtained through this evolutionary process.

## 3. Neural networks for impact location

The second algorithm used for impact location is a mapping procedure based on artificial neural networks (ANNs). ANN is a computer algorithm that emulates the human brain in performing a particular function, i.e. remembering, thinking or problem solving. ANN modelling is applied to predict the system output from given input data. The ability to learn from its environment is one of the major

attributes of the ANN. Two types of learning paradigms are usually adopted in neural network, i.e. supervised and unsupervised learning. The back-propagation algorithm is used to train ANNs in order to produce a desired mapping relationship. The back-propagation learning algorithm involves a forward propagation step followed by backward propagation step. At each training stage, a set of inputs is passed forward through the network to produce a set of outputs. These outputs are then compared to the desired outputs for an error calculation. If a minimum error criterion is not yet achieved, the error is passed backward for connection weight adjustment. This process continues for some time until a minimum error value is obtained.

In this paper, the Multi-Layer Perceptron (MLP) network is chosen to perform regression analysis. The entire algorithm is very straightforward. The MLP works in a multi-layer, feed-forward structure and consists of a series of connected nodes arranged in layers; i.e. input, hidden and output layers. The MLP process starts as the input patterns enter at the input layers ($x_1, x_2 \ldots, x_n$) units. These input patterns progress forward through the hidden layers and the results emerge at the output layer as an output pattern. The hyperbolic tangent was used as the activation function in the entire neural network.

For a given impact the network inputs are signal features obtained from impact strain data whereas the network outputs are estimated $x$ and $y$ coordinates of the impact. The signal features used in the current work are the maximum, minimum, peak-to-peak and variance values calculated in the time domain and the arithmetic mean values for the absolute, real and imaginary spectra calculated in the frequency domain. These parameters were successfully selected following rigorous investigations described in Mahzan (2007). Flexural strain waves, resulting from impact events, were captured by a network of sensors.Three different sets of strain data were collected for the MLP procedure.

The MLP network started with a training stage. At this stage, the architecture of the network was also established to determine the optimum number of hidden units with the corresponding sets of connection weights. This stage utilised data features from the training set and corresponding target output values. The connection weights are iteratively adjusted until the network produces the best match for the actual impact positions. Several training sessions with different initial weights are required for each given network architecture. Once the network was established after the training stage, the next step was applied to validate the network. At this stage, a point at which the training stage should stop was determined. It is because networks which are over-trained learn details of the training data rather than the underlying input-output mapping. Once the optimal network was constructed and validated, the testing data feature set was used to estimate the impact locations.

## 4. Experimental tests

### *4.1. Aircraft wing-box structure*

The test specimen used in the experimental work performed for impact location was a substantial composite wing-box structure. Figs. 4 and 5 give photographs of the entire structure together with a schematic diagram of its cross-section.The structure was a section of one of the flaps taken from a commercial aircraft. The width and length of the structure were equal approximately to 960 and 660 mm, respectively.

The structure had a complex geometry and was manufactured from different materials. The composite skin of the wing-box was curved at the top. The interior of the component below the leading and trailing edges were filled with aramid fibre and aluminium honeycombs, respectively.The underside of

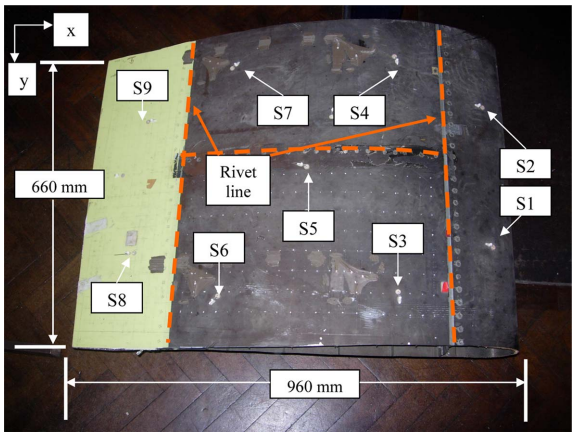


Fig. 4 Composite aircraft wing-box structure used for impact damage location

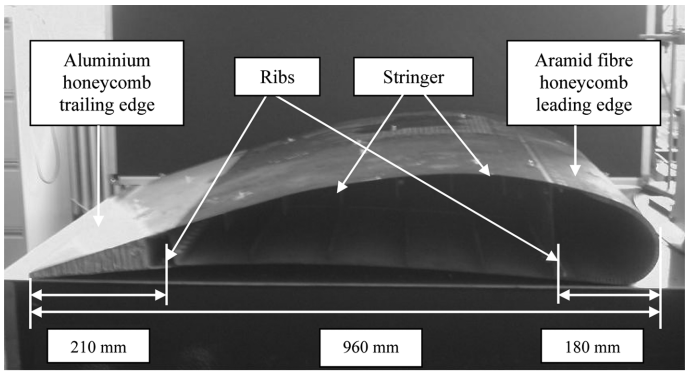


Fig. 5 Cross-section of the composite aircraft wing-box structure

the central area had numerous stringers attached.Vertical and horizontal lines of rivets can be observed at the top curved surface of the structure in Fig. 4. These lines also indicate positions where underside ribs and spars were attached.

The composite structure was instrumented with nine *Sonox-P5* piezoceramic sensors bonded on the top surface. The diameter and thickness of each sensor was equal to 6.5 and 0.25 mm, respectively. The sensors positions, indicated as S1, S2,…, S9 in Fig. 4, are given in Table 1; two sensors were bonded on the leading edge; two on the trailing edge and five in the central area.

### *4.2. Strain wave velocity characteristics*

The first test performed was the experimental analysis of impact strain waves for various wave propagation directions in the composite structure. The objective was to obtain wave velocity characteristics for impact location based on the modified triangulation procedure.The structure, positioned on foam, was divided into four different zones and impact tests were performed separately within each zone.

The analysed zones were: the upper part of the central area (zone 1), the lower part of the central area (zone 2), the trailing edge (zone 3) and the leading edge (zone 4), as illustrated in Fig. 6. It is clear that wave propagation within this zone is different due to variety of material and geometric properties. The

Table 1 Sensor location coordinates on the composite wing-box structure

| Sensors | *x*-coordinate [mm] | *y*-coordinate [mm] |
|---|---|---|
| S1 | 868 | 470 |
| S2 | 868 | 150 |
| S3 | 667 | 577 |
| S4 | 670 | 58 |
| S5 | 485 | 325 |
| S6 | 317 | 588 |
| S7 | 305 | 70 |
| S8 | 115 | 494 |
| S9 | 105 | 182 |

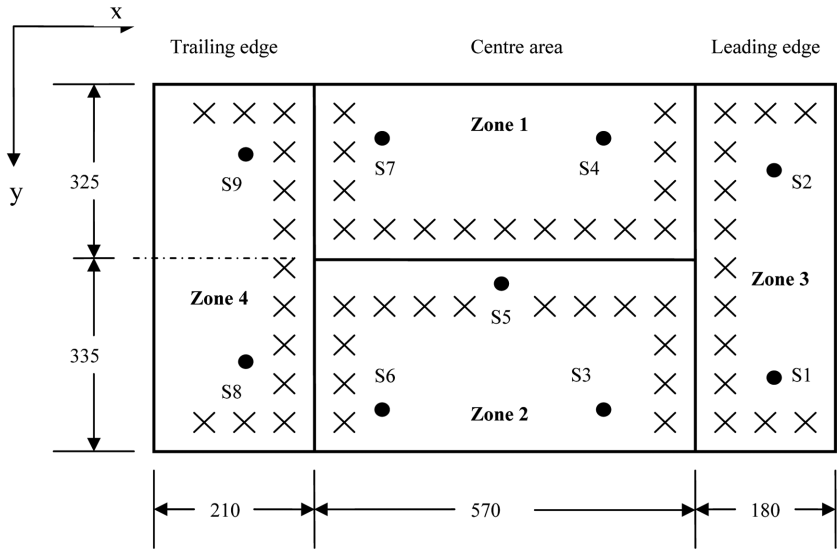


Fig. 6 A schematic diagram showing 4 zones used for impact location investigations in the aircraft composite structure. All dimensions are given in mm. × - impact positions; $S_i$ ($i$=1,2,…,8) - sensor locations

surfaces of zones 1, 2 and 4 are relatively flat when compared with zone 3 which follows the curvature of the leading edge. It is also expected that the level of wave attenuation in zones 3 and 4 is larger if compared with zones 1 and 2 due to honeycomb inserts in the leading and trailing edges.

A series of 41 low-velocities, low-energy impacts were performed at potions indicated in Fig. 6. The resulting strain waves of 2 s were acquired by sensors S4 and S7 in zone 1, sensors S3 and S6 in zone 2, sensors S1 and S2 in zone 3 and finally sensors S8 and S9 in zone 4. The impact strain data were acquired using the *Waverunner LeCroy LT-264* oscilloscope. The sampling frequency used was equal to 5 kHz. The strain data were stored on a PC's hard disc for further analysis. Fig. 7 gives examples of impact strain data from sensors S3 and S7 in response to the impact at $x$=365 mm and $y$=505 mm.

The strain data were used to obtain the wave velocity characteristics. Firstly, the arrival time was estimated for all recorded signals. Then, for known distances between impact and sensor positions, the velocity was calculated from Eq. (1) for the $0\text{-}180^0$ range of wave propagation angles. Fig. 8 shows the strain wave velocity characteristics for all four analysed zones of the aircraft wing-box structure.

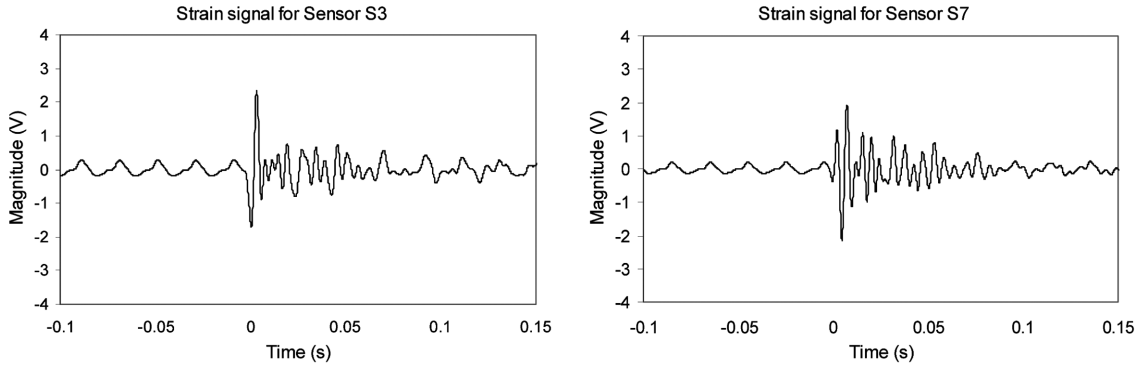


Fig. 7 Examples of strain wave signals acquired by sensors S3 and S7 for impact performed at $x$=365 mm and $y$=505 mm

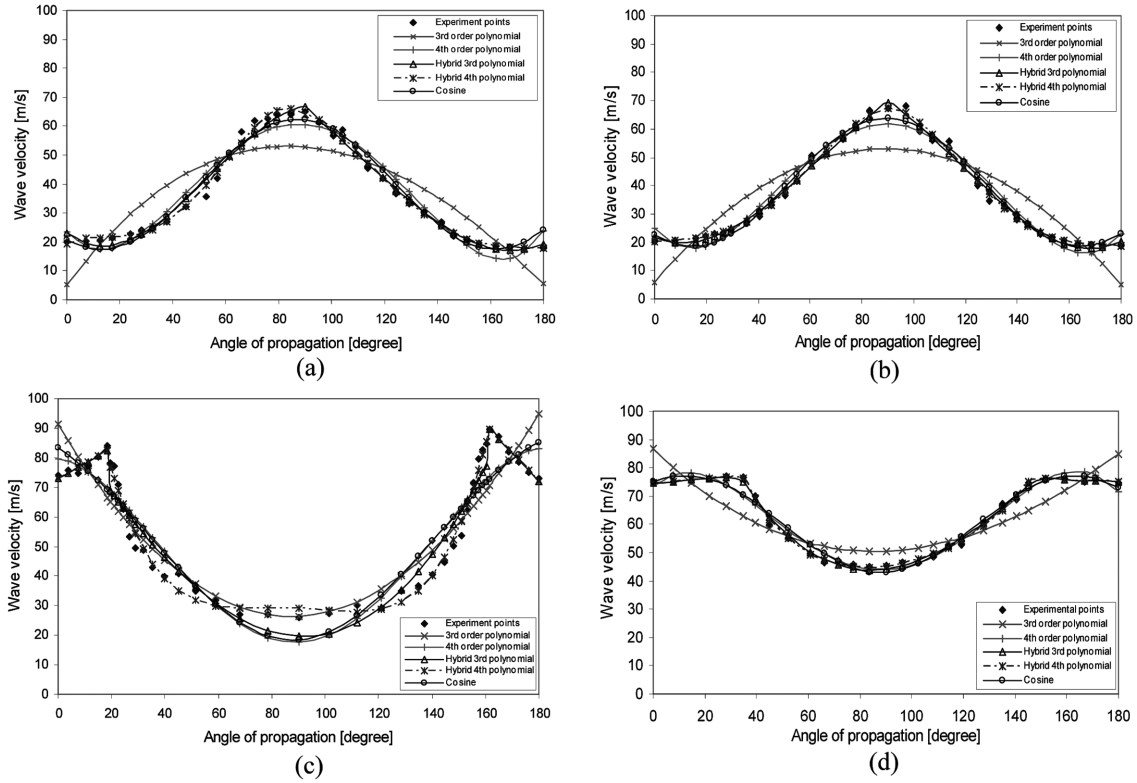


Fig. 8 Wave velocity characteristics for the aircraft wing-box structure produced for the 0°-180° angle range in: (a) zone 1 (b) zone 2 (c) zone 3 (d) zone 4

A curve fitting procedure was applied to the experimental velocity characteristics. Five different analytical functions were used for the curve-fitting. Table 2 shows the examples of relevant functions defined for zone 1. For zone 1 and 2, 4$^{th}$ order polynomials were fitted to the experimental curve for the 0°-90° and 90°-180° angles. For zone 3, the 4$^{th}$ order polynomial was fitted to the experimental curve between 20° and 160° and a straight line was fitted for the remaining part of the curve (i.e. for 0-20° and 160-180°). For zone 4, the 4$^{th}$ order polynomial was fitted to the experimental curve between 35° and

Table 2 Analytical functions used for curve-fitting the zone 1 wave velocity characteristics

| Function | Equation | $a_1$ | $a_2$ | $a_3$ | $a_4$ | $a_5$ | Remarks |
|---|---|---|---|---|---|---|---|
| 1 | $f(x) = a_1x^3 + a_2x^2 + a_3x + a_4$ | 1.473 | -16.16 | -4.185 | 52.73 | - | - |
| 2 | $f(x) = a_1x^4 + a_2x^3 + a_3x^2 + a_4x + a_5$ | 10.43 | 1.352 | -43.2 | -3.94 | 60.59 | - |
| 3 | $f(x) = a_1 + a_2*\cos((x/a_3) + a_4)$ | 39.95 | 22.56 | 0.450 | 0.119 | - | - |
| 4 | $f(x) = a_1x^3 + a_2x^2 + a_3x + a_4$ | 1.82 | 4.435 | -19.92 | 31.46 | - | For angles 0°-90° |
| | | -4.009 | 3.921 | 24.51 | 36.36 | - | For angles 90°-180° |
| 5 | $f(x) = a_1x^4 + a_2x^3 + a_3x^2 + a_4x + a_5$ | -1.234 | 2.113 | 7.436 | -20.23 | 30.58 | For angles 0°-90° |
| | | -3.677 | -4.879 | 12.2 | 25.45 | 33.65 | For angles 90°-180° |

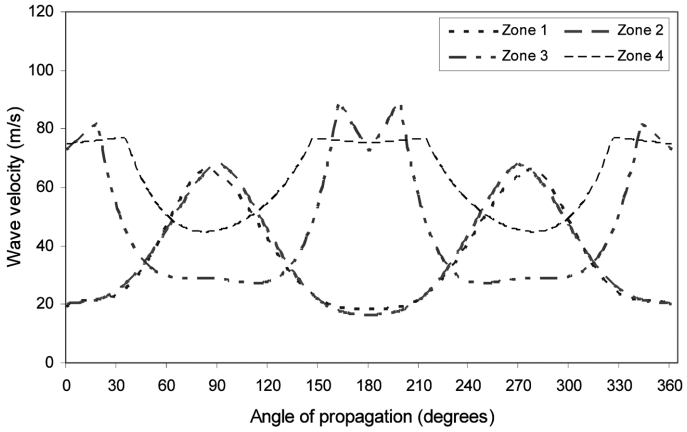


Fig. 9 Wave velocity characteristics for the composite aircraft structure produced for the 0-360° angle range and four analysed zones

145° and the straight line was fitted for the remaining part of the curve (i.e. for 0-35° and 145-180°).

The Mean Square Error (MSE) was used to assess the performance of the functions used for curve fitting. The MSE was defined as

$$MSE(u) = \frac{100}{N\sigma_u^2}\sum_{i=1}^{N}(u_i - \hat{u}_i)^2 \tag{3}$$

where $u_i$ are experimentaldata points, $\hat{u}_i$ are theoretical data points given by the functions used for curve fitting, $\sigma_u$ is the standard deviation of the experimental data and $N$ is the total number of points in the data sets used. The MSE was smaller than 1.4% for all four analysed zones.

Finally, the wave velocity characteristics for the 0-180$^0$ angle range were mirrored (due to the symmetry of the structural layout) to produce the final characteristics for the 0-360° angle range. The final results, presented in Fig. 9 for all analysed zones, were used for further impact location studies based on the modified triangulation procedure. The experimental results show that the wave velocity characteristics are similar for zone 1 and 2, as expected.

### *4.3. Impact tests*

The second series of impacts was performed on the aircraft composite structure to collect the data for the ANN-based impact location procedure. The experimental equipment, set-up, procedure and data

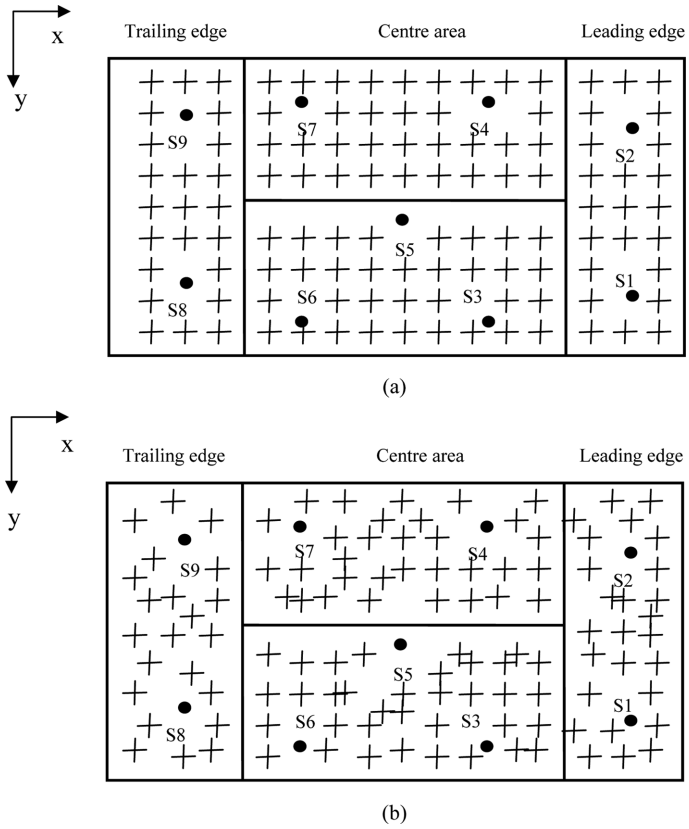


Fig. 10 Impact positions (indicated by crosses) for the aircraft composite wing-box structure: (a) regular grid (b) random grid. Sensors indicated by black filled circles

acquisition parameters were the same as described in Section 5.2. Strain signals were collected for impacts performed on a regular grid and at random positions on the structure. Fig. 10 shows sensor locations and impact positions. Impact positions were characterised using $x$ and $y$ coordinates. For zone 1, impacts were performed on a regular 30×60 mm grid. The total number of impacts was equal to 425 of which 255 events were from the regular grid and the remaining events were from random positions. For zone 2, a regular 25×40 mm grid was used and resulted in the total number of 420 impacts; 280 impact events were performed on the regular grid. For zone 3, a grid size of 30 × 40 mm was applied. In total 420 impacts were introduced, of which 252 events were produced on the regular grid. For zone 4, the size of the regular grid was set to 25×25 mm. The regular grid marking produced 312 impacts from a total of 468 impact events. All these figures are summarised in Table 3. Altogether 1733 strain wave

Table 3 Summary of impact events applied to analysed zone of the aircraft composite wing-box structure

| Zone | Regular Grid Size (in mm) | Total number of impacts | Impacts (Regular Grid) | Impacts (Random) |
|---|---|---|---|---|
| 1 | 30 × 60 | 425 | 255 | 170 |
| 2 | 25 × 40 | 420 | 280 | 140 |
| 3 | 30 × 40 | 420 | 252 | 168 |
| 4 | 25 × 25 | 468 | 312 | 156 |

signals were collected. The mean value was removed from all signals. The data was low-pass filtered to remove undesired noise. The cut-off frequency was equal to 1 kHz.

## 5. Impact location results

### 5.1. Modified triangulation procedure

The first method used followed the algorithm described in Section 3. This algorithm requires the GA optimisation scheme for impact location. The GA used for impact location required encoding of impact coordinates and selection of genetic parameters. The binary and integer encoding (Coverley and Staszewski 2002, 2003, Mahzan 2007) were used to represent three unknown values of wave propagation angles. Three random numbers were chosen to represent angle values. For $i$=1 (sensor $S_1$) and $i$=3 (sensor $S_3$) the actual angle values from the velocity characteristics were taken as $\alpha = \alpha_1+180^0$ and $\alpha = \alpha_3+270^0$, respectively (see Fig. 1). For the binary encoding GA one chromosome consisted of 21 genes. The first seven genes gave the first angle $\alpha_1$, the next seven genes gave the second angle $\alpha_2$ and the last seven genes gave the third angle $\alpha_3$. Seven 0, 1 genes can give a maximum integer number equal to 127 whereas the maximum angle required was between 0 and 90. Therefore, if a random number was greater than 90 the software mapped numbers between 91 and 127 into the set between 0 and 90.

Once a population of chromosomes was selected randomly, the experimental wave velocity characteristics were used to estimate impact positions. The GA was then performed to evolve the initial population and optimise the final impact positions. The entire procedure was coded in *C* and run under *Solaris v.8* operational system. A *Sun* grid computer was used in all calculations. Since there is very little guidance in the literature regarding the choice of GA parameters, a trial and error approach was used for selection. The parameters selected are summarised in Table 4.

The performance of the GA operation was monitored through the maximum and mean fitness values. The natural fitness measure was introduced as the inverse of the total length comprising of lengths $A_1A_2$, $A_1A_3$ and $A_2A_3$ (see Fig. 1).

$$f = \frac{1}{A_1A_2 + A_1A_3 + A_2A_3} \tag{4}$$

Although the GA procedure was run for 500 generations, Fig. 11 demonstrates that both parameters converged after 20 generations for zones 1-2 and 40 generations for zones 3-4 when binary encoding was used. A similar convergence was observed for the integer encoding. This fast convergence was concurrent with the good predictions in impact locations.

Table 4 Summary of GA parameters used for the optimisation scheme

| Parameter name | Binary encoding | Integer encoding |
|---|---|---|
| No of chromosomes per population | 40 | 16 |
| No of generations | 500 | 800 |
| No of genes per chromosome | 21 | 3 |
| Probability of crossover | 0.7 | 0.6 |
| Probability of mutation | 0.05 | 0.01 |
| No of elite chromosomes | 4 | 3 |
| No of new blood chromosomes | 8 | 5 |

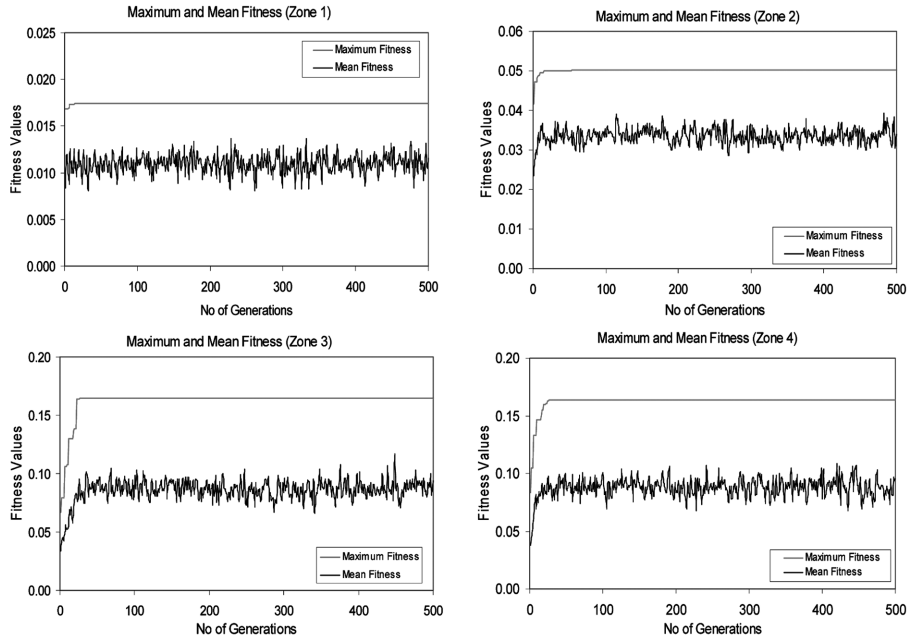


Fig. 11 Maximum and mean fitness values for all analysed zones and binary encoding used

Fig. 12 gives an example of impact location results for the analysed zones when binary encoding was used. The results present the comparison between the actual and estimated impact locations. The results show that although the overall trends of the actual location curves are followed by the estimated location curves, there exist discrepancies in $x$ and $y$ coordinate estimates. Table 5 gives a summary of impact estimation errors for the binary and integer encoding used. This illustrates that the type of encoding had very little influence on the results. Altogether, the errors obtained were smaller than 2% for all analysed structural zones. Zone 1 and 3 gave the best results.

### 5.2. Neural networks

The second method used was based on the ANN algorithm. The *NETLAB* software (Nabney 2002, website:http://www.ncrg.aston.ac.uk/netlab), run on a *PC*, was used for the MLP modelling procedure. The network was designed and trained following the regression algorithm described in Section 4. The back-propagation algorithm was used for training. One hidden layer of 25 elements was used in the computations. The output of the network gave $x$ and $y$ impact coordinates. Seven different networks were designed initially for seven different signal features, described in Section 4. Thus all networks were fed initially with 7 parameters. In the second step the network was fed with all 63 parameters (seven features for strain data from nine sensors). Once the structure of the network was established, validation and testing was performed. This led to the final estimated results which were compared with the actual impact coordinates. Fig. 13 gives an example of impact location results for analysed zones when the network trained on peak-to-peak values. The results show that the overall trend for $x$ and $y$ estimated coordinates is kept if compared with the relevant actual coordinates. However, numerous discrepancies can be observed. These were analysed using the same error parameters as in Section 5.1. A summary of estimation errors for all signal features used is given in Table 6.

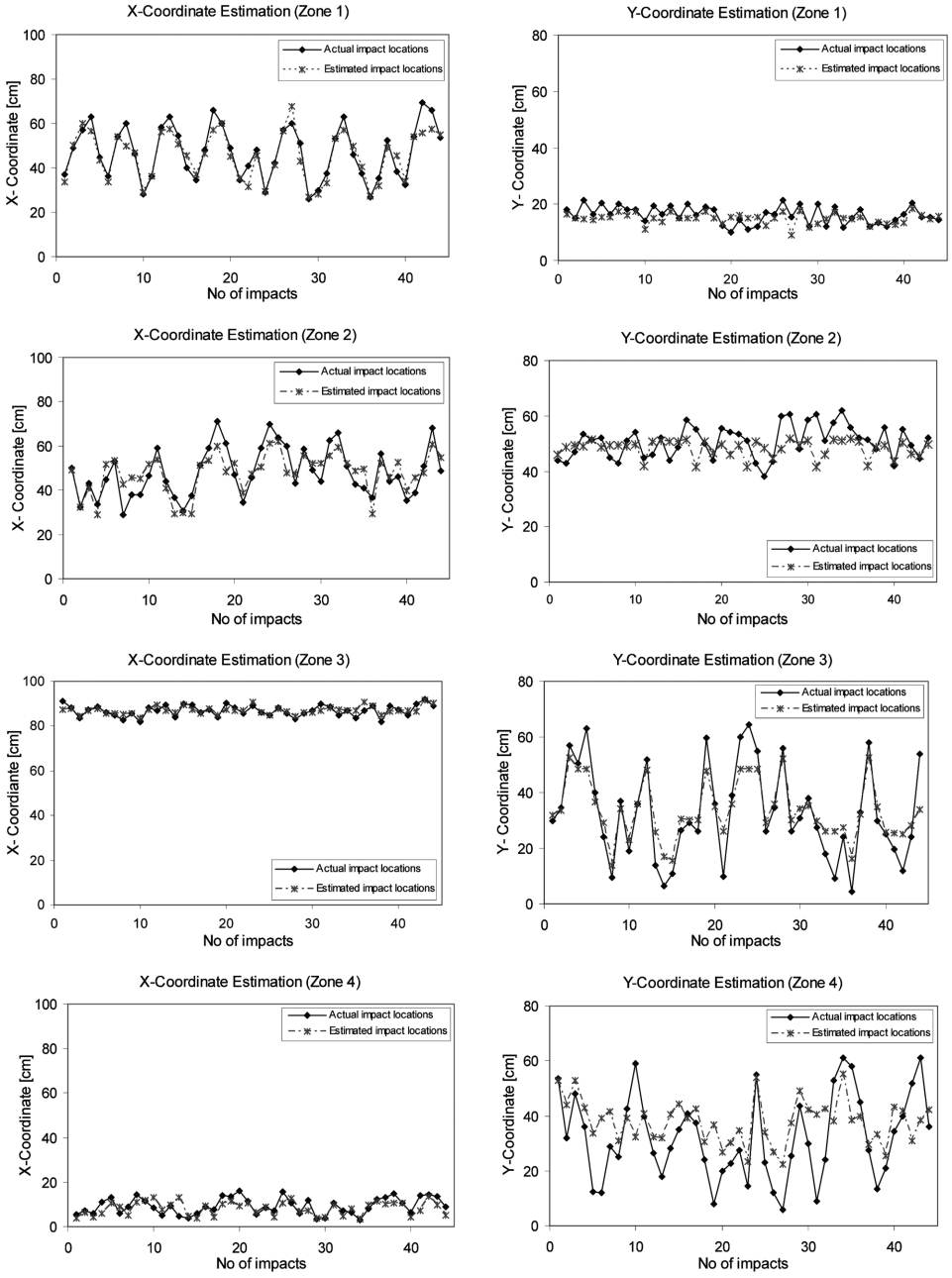


Fig. 12 Modified triangulation procedure with the GA optimisation - examples of impact location estimates for all analysed zones

Altogether, the ANN-based algorithm resulted in impact estimation errors were smaller than 4.3% for all analysed structural features and zones. The study shows that when the network was trained on a single feature, the peak-to-peak value outperformed the other parameters. When the network was trained with all features, the results were improved significantly only for zone 2. The error for all

Table 5 Impact estimation percentage error for the modified triangulation procedure with the GA optimisation

| Zone | Binary encoding | Integer encoding |
|---|---|---|
| Zone 1 | 0.42 | 0.45 |
| Zone 2 | 1.48 | 1.48 |
| Zone 3 | 0.85 | 1.32 |
| Zone 4 | 2.00 | 1.97 |

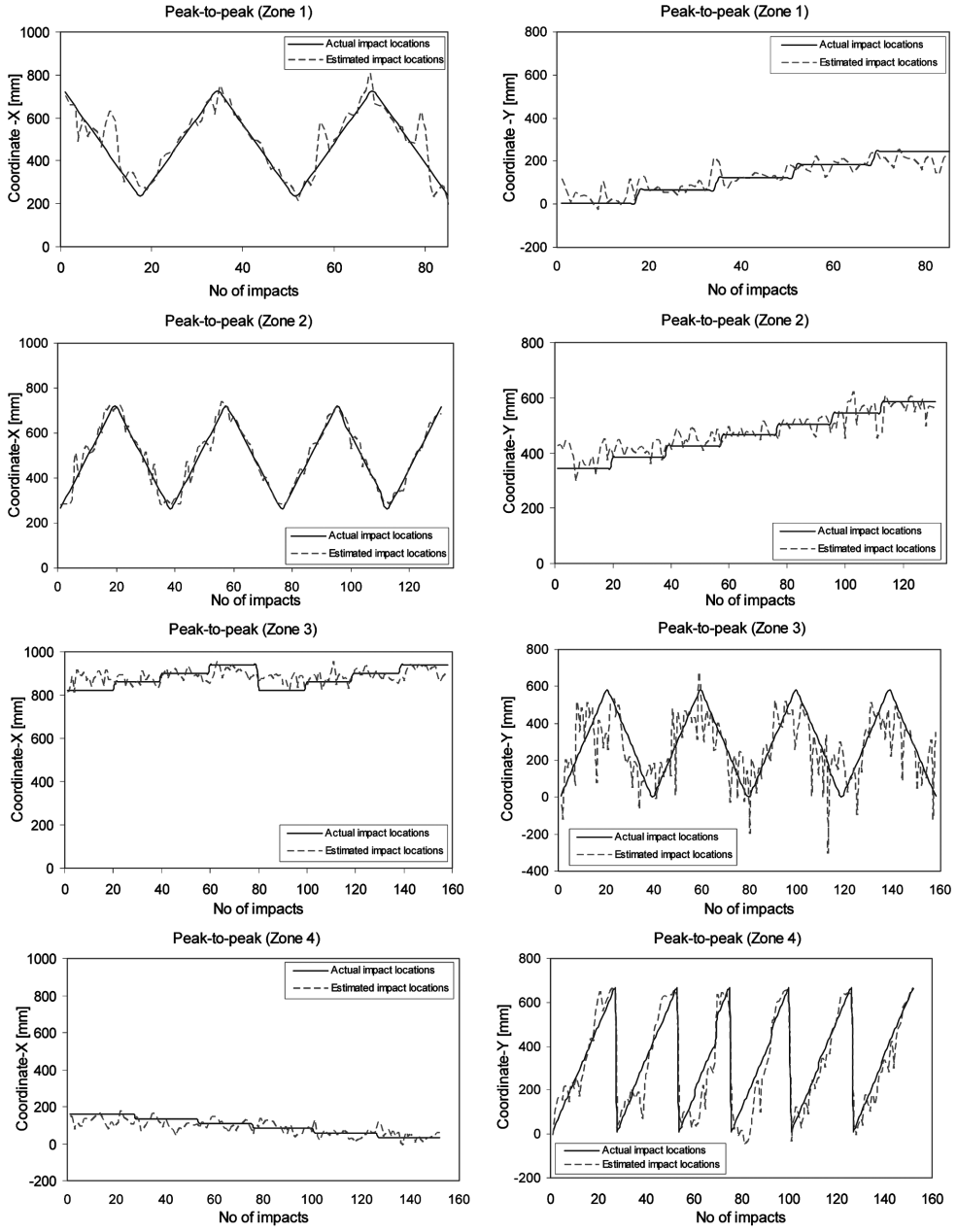


Fig. 13 ANN analysis - examples of impact location estimates when peak-to-peak value is used for analysed zones

Table 6 Impact estimation percentage error for the ANN-based procedure

| Feature | Zone 1 | Zone 2 | Zone 3 | Zone 4 |
|---|---|---|---|---|
| Maximum peak | 0.81 | 0.81 | 3.51 | 1.35 |
| Minimum peak | 0.81 | 0.71 | 3.72 | 1.73 |
| Peak-to-peak | 0.67 | 0.38 | 3.00 | 1.21 |
| Variance | 1.87 | 1.57 | 4.30 | 2.04 |
| Arithmetic mean (absolute spectrum) | 1.06 | 0.34 | 3.11 | 1.91 |
| Arithmetic mean (real spectrum) | 0.72 | 0.42 | 2.71 | 1.70 |
| Arithmetic mean (imaginary spectrum) | 1.29 | 1.14 | 3.59 | 1.92 |
| All features | 0.69 | 0.51 | 2.39 | 1.27 |

features was less than 2.4% for all zones analysed. Zone 1 and 2 gave the best results and the errors were equal to 0.69% and 0.51%, respectively when all features were used for training.

## 6. Conclusions

The experimental study on impact location in the aircraft composite structure was performed using the modified triangulation procedure with the GA optimisation scheme and the ANN-based procedure. Both procedures resulted in good impact location estimates. The estimation errors are of the same order and smaller than 2% for the modified triangulation procedure with the GA optimisation scheme and smaller than 2.4% for the ANN-based procedure with all features used for training. There is very little difference between the binary and integer encoding used in the modified triangulation procedure. When the ANN-based procedure is used, the results are improved significantly only for zone 3 when all features are used for training.The ANN-based procedure has produced the best results (impact estimation errors smaller than 0.7% when peak-to-peak values or all features used for training) for the central zones (1 and 2) of the composite structure. This result was expected since these zones were not filled with core inserts which cause significant wave attenuation. In contrast, the modified triangulation procedure has produced the best results (impact estimation errors smaller than 0.9% when the binary encoding used) for zones 1 and 3. This needs further investigations, as the result for zone 2 was expected to be better than for zone 3, as explained above.

In summary, the modified triangulation procedure with the GA optimisation scheme produces similar results as the ANN-based procedure. The advantage of the modified triangulation procedure is that it does not require substantial data. However, it is more computationally expensive when tested for impact location. Once the network is learned and validated, the ANN-based procedure is very fast and produces immediate impact location results. Although both methods offer a good solution to the impact detection problem further comparative tests are required to confirm the findings in this paper. This work should investigate higher energy impacts which damage analysed structures.

The question remains whether simulation data (i.e. wave velocity characteristics in the modified triangulation procedure and impact strain data used for training and validation in the ANN-based procedure) could be used in practical application. The study should also address the problem of different signal features in the ANN-based algorithm. All these elements will be the subject of future investigations.

## Acknowledgement

The first author was supported by a grant from the University of Tun Hussein Onn in Malaysia once studying for a PhD at the University of Sheffield.

## References

Cardi, A.A., Adams, D.E. and Walsh, S. (2006), "Ceramic body armor single impact identification on a compliant torso using acceleration response mapping", *Struct. Health Monit.*, **5**(4), 355-372.

Choi, K. and Chang, F.K. (1996), "Identification of impact force and location using distributed sensors", *American Institute of Aeronautics and Astronautics J.*, **34**(1), 136-142.

Coverley, P.T. and Staszewski, W.J. (2002), "Impact damage location in composite structures using genetic algorithms", *Proc. of the 1st European Workshop on Structural Health Monitoring*, Paris, France, 271-278.

Coverley, P.T. and Staszewski, W.J. (2003), "Impact damage location in composite structures using optimized sensor triangulation procedure", *Smart. Mater. Struct.*, **12**, 1-9.

Gardiner, D.S. and Pearson, L.H. (1985), *Acoustic emission monitoring of composite damage under static and impact loading*, Technical report, Hercules Aerospace Co. Magna UT.

Goldberg, D.E. (1989), *Genetic algorithms in search optimisation, and machine learning*, Reading, MA, Addison-Wesley.

Gunther, M.F., Wang, A., Fogg, R.P., Starr, S.E., Murphy, K.A. and Claus, R.O. (1992), "Fibre optic impact detection and location system embedded in a composite material", *SPIE Proc. of the Fibre Optic Smart Structures and Skins IV*, **1588**, 64-75.

Hahn, H.T., Wilkerson, B. and Stuart, J. (1994), "An artificial neural network for low-energy impact monitoring", *J. Thermoplast. Compos.*, **7**(4), 344-351.

Haywood, J., Coverley, P.T., Staszewski, W.J. and Worden, K. (2005), "An automatic impact monitor for a composite panel employing smart sensor technology", *Smart. Mater. Struct.*, **14**, 1-7.

Haywood, J., Staszewski, W.J. and Worden, K. (2001), "Impact location in composite structures using smart sensor technology and neural networks", *Proc. of the 3rd Int. Workshop on Structural Health Monitoring*, Stanford, California, 1466-1475.

Holland, J.H. (1975), *Adaptation in natural and artificial systems*, University of Michigan Press, Ann Arbor.

Kessler, S.S. and Raghavan, R. (2008), "Vector-based localization for damage position identification from a single SHM node", *Proc. of the 1st Int. Workshop on Prognostics & Health Management*, Denver, Colorado, 6-9 October.

Le Clerc, J.R., Worden, K., Staszewski, W.J. and Haywood, J. (2004), "Impact detection in an aircraft composite panel - a neural network approach", *Proc. of the 2nd European Workshop on Structural Health Monitoring*, Munich, Germany, 407-414.

Le Clerc, J.R., Worden, K., Staszewski, W.J. and Haywood, J. (2007), "Impact detection in an aircraft composite panel - a neural-network approach", *J. Sound Vib.*, **299**, 672-682.

Mahzan, S. (2007), *Impact location in composite structures using advanced signal processing procedures*, PhD thesis, Department of Mechanical Engineering, University of Sheffield.

Meo, M., Zumpano, G., Piggott, M. and Marengo, G. (2005), "Impact identification on a sandwich plate from wave propagation response", *Compos. Struct.*, **71**, 302-306.

Mujica, L.E., Vehi, J., Ruiz, M.L., Verleysen, M., Staszewski, W.J. and Worden, K. (2008), "Multivariate statistics process control for dimensionality reduction in structural assessment", *Mech. Syst. Signal Pr.*, **22**(1), 155-171.

Mujica, L.E., Vehi, J., Staszewski, W.J. and Worden, K. (2005), "Impact damage detection in aircraft composites using knowledge-based reasoning", *Proc. of the 5th Int. Workshop on Structural Health Monitoring*, Stanford, California.

Mujica, L.E., Vehi, J., Staszewski, W.J. and Worden, K. (2008), "Impact damage detection in aircraft composites using knowledge-based reasoning", *Struct. Health Monit.*, Online doi:10.1177/1475921708090560.

Mujica, L.E., Vehi, J., Staszewski, W.J. and Worden, K. (2006), "Multivariate statistics process control for dimensionality reduction on structural health monitoring", *Proc. of the 3rd European Workshop on Structural Health Monitoring*, Granada, Spain, 601-608.

Nabney, I.T. (2002), *Netlab: algorithms for pattern recognition*, Springer.

Schindler, P.M., May, R.M., Claus, R.O. and Shaw, J.K. (1995), "Location of impacts in composite panels by embedded fibre optic sensors and neural network processing", *SPIE Proc. of the Smart Structures and Materials Symp*, Smart Sensing, Processing and Instrumentation, **2444**, 481-490.

Seydel, R. and Chang, F.K. (2001), "Impact identification of stiffened composite panels: I. System development", *Smart Mater. Struct.*, **10**, 354-369.

Seydel, R. and Chang, F.K. (2001), "Impact identification of stiffened composite panels: II. Implementation studies", *Smart Mater. Struct.*, **10**, 354-369.

Seydel, R. and Chang, F.K. (1999), "Real-time impact identification of stiffened composite panels", *SPIE Proc. of the Smart Structures and Materials*, Newport Beach, California, **3668**(1), 295-305.

Sirkis, J.S., Shaw, J.K., Berkoff, T.A., Kersey, A.D., Fribele, E.J. and Jones, R.T. (1994), "Development of an impact detection technique using optical fiber sensor and neural networks", *SPIE Proc. of the Smart Structures and Materials Symposium*, Smart Sensing, Processing and Instrumentation, **2191**, 158-165.

Staszewski, W.J., Boller, C. and Tomlinson, G.R. (1999), "Impact damage detection in composite structures - recent advances", *Proc. of the 2nd Int. Workshop on Structural Health Monitoring*, Stanford, California, 754-763.

Staszewski, W.J., Boller, C.B.C. and Tomlinson, G.R. (2002), "Impact damage detection in composite structures using passive acousto-ultrasonic sensors", *Key Engineering Materials*, **221-222**, 389-400.

Staszewski, W.J., Worden, K., Wardle, R. and Tomlinson, G.R. (2000), "Fail-safe sensor distributions for impact detection in composite materials", *Smart. Mater. Struct.*, **9**, 298-303.

Sung, D.U., Oh, J.H., Kim, C.G. and Hong, C.S. (2000), "Impact monitoring of smart composite laminates using neural network and wavelet analysis", *J. Intel. Mat. Syst. Str.*, **11**, 180-190.

Website, http://www.ncrg.aston.ac.uk/netlab.

Weems, D., Hahn, H.T., Granlund, E. and Kim, I.G. (1991), "Impact detection in composite skin panels using piezoelectric sensors", *Proc. of the 47th Annual Forum of the Americal Helicopter Society.*

Worden, K. and Staszewski, W.J. (2000), "Impact location and quantification on a composite panel using neural networks and a Genetic Algorithm", *Strain*, **36**(2), 61-70.